

Valid inference after prediction

Keshav Motwani

Department of Biostatistics, University of Washington,

Daniela Witten

Departments of Biostatistics and Statistics, University of Washington

June 27, 2023

Abstract

Recent work has focused on the very common practice of prediction-based inference: that is, (i) using a pre-trained machine learning model to predict an unobserved response variable, and then (ii) conducting inference on the association between that predicted response and some covariates. As pointed out by Wang et al. [2020], applying a standard inferential approach in (ii) does not accurately quantify the association between the unobserved (as opposed to the predicted) response and the covariates. In recent work, Wang et al. [2020] and Angelopoulos et al. [2023] propose corrections to step (ii) in order to enable valid inference on the association between the unobserved response and the covariates. Here, we show that the method proposed by Angelopoulos et al. [2023] successfully controls the type 1 error rate and provides confidence intervals with correct nominal coverage, regardless of the quality of the pre-trained machine learning model used to predict the unobserved response. However, the method proposed by Wang et al. [2020] provides valid inference only under very strong conditions that rarely hold in practice: for instance, if the machine learning model perfectly approximates the true regression function in the study population of interest.

1 Introduction

Rapid recent progress in the field of machine learning has enabled the development of complex and high-quality machine learning models to predict a response variable of interest. This is particularly attractive in settings where future measurement of this response variable is prohibitively expensive or impossible. For example, instead of performing expensive experiments to determine a protein’s structure, it is possible to obtain high-quality structural predictions using AlphaFold [Jumper et al., 2021]. Similarly, in developing countries, determining the true cause of death may be impossible; instead, one might predict the cause of death on the basis of a “verbal autopsy” [Clark et al., 2015, Khoury et al., 1999]. In the context of gene expression data, it is infeasible to conduct experiments in every possible tissue type, and so instead a machine learning model can be applied to predict gene expression in a tissue type of interest [Ellis et al., 2018, Gamazon et al., 2015, Gusev et al., 2019].

In this paper, we will use the notation $\hat{f} : \mathcal{Z} \rightarrow \mathcal{Y}$ to denote a pre-trained machine learning model that maps from \mathcal{Z} , the space of the predictors Z , to \mathcal{Y} , the space of the response variable Y . We assume that the operating characteristics of $\hat{f}(\cdot)$ in the study population of interest are

unknown to the end-user, and the data used to fit $\hat{f}(\cdot)$ are unavailable. Thus, in what follows, we will treat $\hat{f}(\cdot)$ as a “black box” function.

In important recent papers, Wang et al. [2020] and Angelopoulos et al. [2023] consider the practice of *prediction-based inference*¹: that is, of quantifying the association between some covariates X and the response Y using realizations not of (X, Y) , but rather, of $(X, \hat{f}(Z))$. Such an approach is attractive in cases where the association between X and Y is of interest, and both $\hat{f}(\cdot)$ and a large sample of realizations of predictors Z and covariates X are available, but realizations of Y are expensive or otherwise unavailable. Throughout, we will use Z to denote the *predictors* in the machine learning model $\hat{f}(\cdot)$, and X to denote the *covariates* whose association with Y is of interest. In many settings, the covariate variables X may be a subset of the predictor variables Z , or may be identical to Z , but this is not necessarily the case.

Wang et al. [2020] point out that a naive approach to prediction-based inference that simplistically interprets the association between $(X, \hat{f}(Z))$ as the association between (X, Y) is problematic from a statistical perspective. For instance, regressing $\hat{f}(Z)$ onto X using least squares does not lead to valid inference on the association between Y and X : e.g. it leads to hypothesis tests that fail to control type 1 error, and confidence intervals that do not achieve the nominal coverage. See Box 1.

Box 1: *Naive approach to prediction-based inference.* We are given a (pre-trained) prediction function $\hat{f}(\cdot) : \mathcal{Z} \rightarrow \mathcal{Y}$, and an unlabeled dataset $\mathbf{z}_{\text{unlab}}$ representing realizations from Z . As pointed out by Wang et al. [2020], the naive approach displayed here does not allow for valid inference on the association between Y and X .

Step 1: Compute $\hat{\mathbf{y}}_{\text{unlab}} = \hat{f}(\mathbf{z}_{\text{unlab}})$.

Step 2: Conduct inference on the association between Y and X , using $\hat{\mathbf{y}}_{\text{unlab}}$ and $\mathbf{x}_{\text{unlab}}$ as data, without accounting for the fact that $(\hat{\mathbf{y}}_{\text{unlab}}, \mathbf{x}_{\text{unlab}})$ is not a sample from the distribution of (Y, X) .

Wang et al. [2020] and Angelopoulos et al. [2023] propose creative solutions to overcome this issue. They assume that in addition to a large unlabeled dataset $(\mathbf{z}_{\text{unlab}}, \mathbf{x}_{\text{unlab}})$, they also have access to a (relatively small) labeled dataset $(\mathbf{z}_{\text{lab}}, \mathbf{x}_{\text{lab}}, \mathbf{y}_{\text{lab}})$. Both the labeled and unlabeled data are samples from the same study population of interest. See Box 2. We emphasize that the goal is to quantify association between Y and X .

One simple (and valid) option is to quantify association between Y and X using only the labeled data $(\mathbf{x}_{\text{lab}}, \mathbf{y}_{\text{lab}})$. However, this approach entirely discards the vast amount of unlabeled data $(\mathbf{z}_{\text{unlab}}, \mathbf{x}_{\text{unlab}})$. Intuitively, if the prediction function $\hat{f}(\cdot)$ is nearly perfect on our population of interest, then using $(\mathbf{x}_{\text{unlab}}, \hat{f}(\mathbf{z}_{\text{unlab}}))$ in addition to $(\mathbf{x}_{\text{lab}}, \mathbf{y}_{\text{lab}})$ will aid our efforts to quantify the association between X and Y . By contrast, if $\hat{f}(Z)$ is a very poor prediction of Y on our population of interest, then using $(\mathbf{x}_{\text{unlab}}, \hat{f}(\mathbf{z}_{\text{unlab}}))$ in addition to $(\mathbf{x}_{\text{lab}}, \mathbf{y}_{\text{lab}})$ may hinder our efforts. Our goal is valid quantification of the association between Y and X , *regardless of the quality of $\hat{f}(\cdot)$ on the population of interest.*

To achieve this goal, Wang et al. [2020] propose to (Step 1’) model the association between Y

¹Wang et al. [2020] and Angelopoulos et al. [2023] refer to this practice as *post-prediction inference* and *prediction-powered inference*, respectively; to unify terminology, here we refer to it as *prediction-based inference*.

Box 2: *Setting of prediction-based inference.*

- *Given:* A pre-trained machine learning model $\hat{f} : \mathcal{Z} \rightarrow \mathcal{Y}$.
- *Goal:* To quantify the association between a response $Y \in \mathcal{Y}$ and covariates $X \in \mathcal{X}$.
- *Data:* A (relatively small) labeled dataset $(\mathbf{z}_{\text{lab}}, \mathbf{x}_{\text{lab}}, \mathbf{y}_{\text{lab}})$ consisting of independent realizations of (Z, X, Y) , and a (large) unlabeled dataset $(\mathbf{z}_{\text{unlab}}, \mathbf{x}_{\text{unlab}})$ consisting of independent realizations of (Z, X) . Both are drawn from the same study population.

and $\hat{f}(Z)$ using the labeled dataset $(\mathbf{z}_{\text{lab}}, \mathbf{y}_{\text{lab}})$, and then (Step 2') incorporate the model in Step 1' to conduct inference between Y and X using the unlabeled data $(\mathbf{x}_{\text{unlab}}, \hat{f}(\mathbf{z}_{\text{unlab}}))$. See Box 3.

Box 3: *Wang et al. [2020]'s proposal to correct prediction-based inference.*

Step 1': Model the association between Y and $\hat{f}(Z)$ using the labeled data $(\mathbf{z}_{\text{lab}}, \mathbf{y}_{\text{lab}})$.

Step 2': Incorporate the model from Step 2' to conduct inference between Y and X using the unlabeled data $(\mathbf{x}_{\text{unlab}}, \hat{f}(\mathbf{z}_{\text{unlab}}))$. To do this, bootstrap and analytical approaches are proposed.

By contrast, Angelopoulos et al. [2023] propose to (Step 1'') compute the difference between the estimate of the parameter of interest obtained using $(\mathbf{x}_{\text{lab}}, \hat{f}(\mathbf{z}_{\text{lab}}))$ to the estimate obtained using $(\mathbf{x}_{\text{lab}}, \mathbf{y}_{\text{lab}})$. They then (Step 2'') correct the estimate obtained using the unlabeled dataset $(\mathbf{x}_{\text{unlab}}, \hat{f}(\mathbf{z}_{\text{unlab}}))$ by this amount. See Box 4.

Box 4: *Angelopoulos et al. [2023]'s proposal to correct prediction-based inference.*

Step 1'': Compute the difference between the estimate of the parameter of interest obtained using $(\mathbf{x}_{\text{lab}}, \hat{f}(\mathbf{z}_{\text{lab}}))$ to the estimate obtained using $(\mathbf{x}_{\text{lab}}, \mathbf{y}_{\text{lab}})$.

Step 2'': Correct the parameter estimate obtained using the unlabeled dataset $(\mathbf{x}_{\text{unlab}}, \hat{f}(\mathbf{z}_{\text{unlab}}))$ by the difference computed in Step 1''.

In this paper, we investigate these two proposals. Using the simulation setting considered in Wang et al. [2020], we show in Section 2 that the proposal by Wang et al. [2020] (Box 3) does not lead, in general, to tests that control the Type 1 error, or confidence intervals that attain the nominal coverage. This issue becomes especially pronounced as the size of the data (both labeled and unlabeled) increases. In Section 3, we show that this issue arises because their estimators are not consistent for the parameter of interest, rendering the assumed distribution used for inference incorrect – especially when the prediction function is poor. However, the proposal of Angelopoulos et al. [2023] (Box 4) results in valid inference, regardless of the quality of the prediction function $\hat{f}(\cdot)$. We close with a discussion in Section 4.

In this paper, we use capitals to represent a random variable and lower case to represent

its realization. Vectors of length equal to the number of observations, or matrices whose rows correspond to the observations, are in bold.

2 Empirical performance of Wang et al. [2020]’s and Angelopoulos et al. [2023]’s proposed corrections

2.1 Overview

We consider the simulation study presented in the “*Simulated Data: Continuous case*” section of Wang et al. [2020]. They generate three datasets in each replicate of the simulation study: a *training dataset* consisting of realizations of (Z, X, Y) used to train a machine learning model $\hat{f}(\cdot)$, a *labeled dataset* consisting of realizations of (Z, X, Y) , and an *unlabeled dataset* consisting only of realizations of (Z, X) ; both the labeled and unlabeled datasets are used for inference². They consider predictors $Z \in \mathbb{R}^4$ and response $Y \in \mathbb{R}$, and define the covariate $X := Z_1$. In Wang et al. [2020]’s paper, the training, labeled, and unlabeled datasets each consist of 300 observations. Throughout this section, we keep the training sample size fixed at 300 observations, but vary the size of the labeled and unlabeled datasets.

In this simulation study, Wang et al. [2020] generate the training, labeled, and unlabeled datasets from the same partially linear additive model $Y = \tilde{\beta}_0 + \tilde{\beta}_1 Z_1 + \sum_{j=2}^4 \tilde{\beta}_j g_j(Z_j) + \epsilon$. Their goal is to conduct inference on the marginal association between $X = Z_1$ and Y in a linear model. That is, their parameter of interest is

$$\beta_1^* = \arg \min_{\beta_0, \beta_1} \mathbb{E}[(Y - \beta_0 - \beta_1 Z_1)^2]. \quad (1)$$

Because the features are independent, we have that

$$\beta_1^* = \arg \min_{\beta_0, \beta_1, \dots, \beta_4} \mathbb{E}[(Y - \beta_0 - \beta_1 Z_1 - \sum_{j=2}^4 \beta_j g_j(Z_j))^2] = \tilde{\beta}_1. \quad (2)$$

Thus, β_1^* is the marginal regression coefficient of Y onto $X = Z_1$, as well as the coefficient associated with $X = Z_1$ in the partially linear additive model used to generate the data.

Following Wang et al. [2020], we fit a generalized additive model to the training set, to obtain the fitted model $y \approx \hat{f}(z)$ ³. To conduct prediction-based inference on β_1^* , we first consider the proposal of Wang et al. [2020].

1. *Proposal of Wang et al. [2020], with an analytical correction.* Apply Box 3 with the “analytical correction” described in Wang et al. [2020].
2. *Proposal of Wang et al. [2020], with a “parametric bootstrap” correction.* Apply Box 3 with the “parametric bootstrap” correction presented in Algorithm 1.
3. *Proposal of Wang et al. [2020], with a “non-parametric bootstrap” correction.* Apply Box 3 with the “non-parametric bootstrap” correction presented in Algorithm 1.

²Wang et al. [2020] refer to the labeled data set as “test” data, and to the unlabeled data as “validation” data.

³Note that this $\hat{f}(\cdot)$ is different for each replicate of the simulation study.

We additionally consider the proposal of Angelopoulos et al. [2023]:

4. *Proposal of Angelopoulos et al. [2023]*. Apply Box 4 using a linear model.

Finally, we consider the following two approaches.

5. *Classical approach using only the labeled data*. Fit a linear model to $(\mathbf{x}_{\text{lab}}, \mathbf{y}_{\text{lab}})$.
6. *Naive approach*. Apply Box 1 using a linear model.

2.2 Type 1 error control

In each of 1,000 simulation replicates, we generated a training, labeled, and unlabeled dataset with $\beta_1^* = 0$. In each simulation replicate, we tested the null hypothesis $H_0 : \beta_1^* = 0$ using each of the approaches described in Section 2.1. Quantile-quantile plots of the resulting 1,000 p-values are shown in Figure 1.

We see that in agreement with the findings in Wang et al. [2020], the naive approach does not control the type 1 error rate. Surprisingly, *the proposals by Wang et al. [2020] also fail to control the type 1 error rate*, especially as the sample sizes increase. We further see that the method proposed by Angelopoulos et al. [2023] controls type 1 error, in support of the theory in Proposition 4 of Angelopoulos et al. [2023], which holds for an arbitrary prediction function $\hat{f}(\cdot)$. As expected, the classical method also controls type 1 error.

In this section, we adopted the simulation set-up of Wang et al. [2020], which involved sampling a new training dataset — and consequently, a new $\hat{f}(\cdot)$ — in each simulation replicate. However, recall that the intended applications of prediction-based inference involve large pre-trained machine learning models $\hat{f}(\cdot)$, such as AlphaFold, which will each be used repeatedly to conduct inference. Thus, in Appendix A, we generate a single $\hat{f}(\cdot)$, and then create new labeled and unlabeled data (but not new training data) within each simulation replicate. We find once again that the proposal of Angelopoulos et al. [2023] controls the Type 1 error, whereas the proposals of Wang et al. [2020] do not.

2.3 Coverage of 95% confidence intervals

In each of 1,000 simulation replicates, we generated a training, labeled, and unlabeled dataset with $\beta_1^* = 1$. In each simulation replicate, we then constructed a 95% confidence interval for the parameter β_1^* , using the approaches described in Section 2.1. While Wang et al. [2020] do not explicitly discuss confidence intervals, they claim that $\hat{\beta}_1 / \widehat{SE}(\hat{\beta}_1) \rightarrow N(0, 1)$ when $\beta_1^* = 0$, where $\widehat{SE}(\hat{\beta}_1)$ is the estimate of the standard deviation obtained in Steps 4 and 5 of Algorithm 1; thus, here we construct confidence intervals for their proposal under the assumption that $(\hat{\beta}_1 - \beta_1^*) / \widehat{SE}(\hat{\beta}_1) \rightarrow N(0, 1)$.

We see from Figure 2 that the naive approach has coverage well below the nominal level. Again, surprisingly, *the “corrected” proposals of Wang et al. [2020] also fail to achieve the nominal coverage*. The problem becomes increasingly pronounced as the sample sizes of the data used for inference increase. By contrast, the classical method and the proposal of Angelopoulos et al. [2023] do achieve the nominal coverage.

In Appendix A, we display coverage in a simulation study that holds $\hat{f}(\cdot)$ fixed across simulation replicates, and generates new labeled and unlabeled data (but not training data) in each simulation

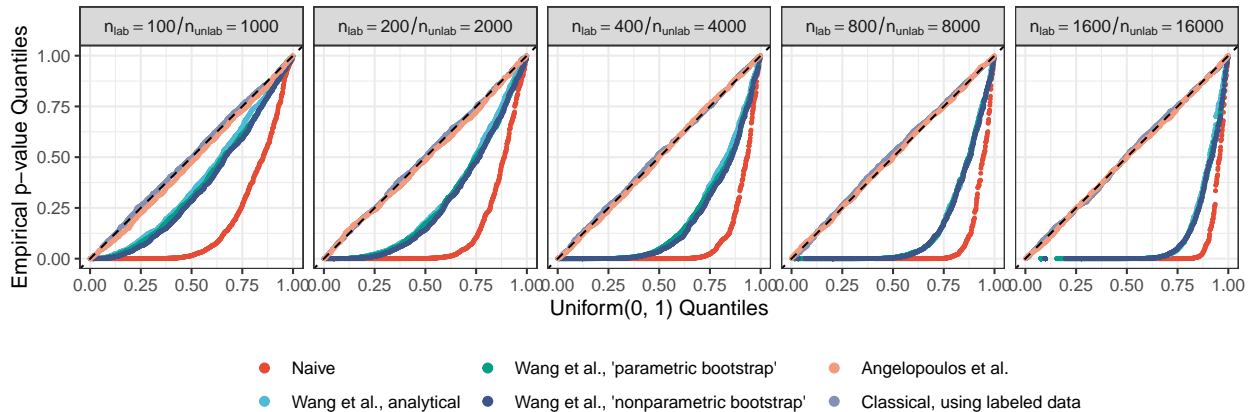


Figure 1: For data generated under $H_0 : \beta_1^* = 0$, quantile-quantile plots of the p-values across simulation replicates are displayed. The methods are described in Section 2.1. Each panel corresponds to a different sample sizes of the labeled and unlabeled datasets used for inference. The bootstrap and analytical corrections considered by Wang et al. [2020] become increasingly anticonservative as the sample sizes increase. The classical approach, and that of Angelopoulos et al. [2023], are well-calibrated.

replicate. The results are quite similar to those seen in Figure 2, and support the theory in Proposition 4 of Angelopoulos et al. [2023].

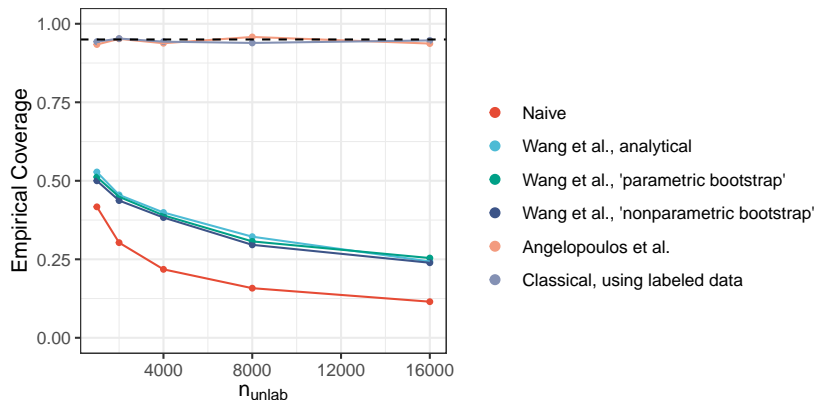


Figure 2: For data generated with $\beta_1^* = 1$, empirical coverage of 95% confidence intervals for each method across each simulation replicate, as the labeled and unlabeled sample sizes increase, with $n_{\text{lab}} = 0.1n_{\text{unlab}}$. The methods are described in Section 2.1.

3 A closer look at the corrections of Wang et al. [2020]

We now investigate why the corrections of Wang et al. [2020] fail to control the type 1 error or achieve the nominal coverage. We begin with an overview of the bootstrap correction in Section 3.1.

Algorithm 1 Bootstrap correction of Wang et al. [2020]. The goal is to conduct inference on the relationship between Y and X .

1. Use $(\mathbf{z}_{\text{lab}}, \mathbf{y}_{\text{lab}})$ to fit the “relationship model” $Y|\hat{f}(Z) \sim K(\hat{f}(Z), \phi)$, yielding $\hat{\phi}$.
 2. For $b = 1, \dots, B$:
 - 2.1. Sample unlabeled observations with replacement to obtain $\mathbf{z}_{\text{unlab}}^b$ and $\mathbf{x}_{\text{unlab}}^b$.
 - 2.2. Sample outcomes $\tilde{\mathbf{y}}^b|\hat{f}(\mathbf{z}_{\text{unlab}}^b)$ from the relationship model $K(\hat{f}(\mathbf{z}_{\text{unlab}}^b), \hat{\phi})$.
 - 2.3. Use $(\mathbf{x}_{\text{unlab}}^b, \tilde{\mathbf{y}}^b)$ to fit a “regression model” for the relationship between Y and X , and record the coefficient estimate $\hat{\beta}^b$ and model-based standard error \hat{s}^b .
 3. Compute the point estimate $\hat{\beta} = \text{median}\{\hat{\beta}^1, \dots, \hat{\beta}^B\}$.
 4. Compute the “nonparametric” standard error $\widehat{\text{SE}}(\hat{\beta}) = \text{SD}\{\hat{\beta}^1, \dots, \hat{\beta}^B\}$.
 5. Compute the “parametric” standard error $\widehat{\text{SE}}(\hat{\beta}) = \text{median}\{\hat{s}^1, \dots, \hat{s}^B\}$.
-

3.1 Overview of the bootstrap correction of Wang et al. [2020]

The bootstrap correction proposed by Wang et al. [2020] is presented in Algorithm 1. Roughly, the idea is as follows. First, a “relationship model” $Y|\hat{f}(Z) \sim K(\hat{f}(Z), \phi)$ is fit to the labeled dataset, in order to model the association between Y and $\hat{f}(Z)$, where $K(\cdot, \cdot)$ is a user-specified distribution with parameter ϕ ; we let $\hat{\phi}$ denote the estimated parameter. Next, the rows of $\mathbf{z}_{\text{unlab}}$ and $\mathbf{x}_{\text{unlab}}$ are sampled with replacement to give $\mathbf{z}_{\text{unlab}}^b$ and $\mathbf{x}_{\text{unlab}}^b$, and $\tilde{\mathbf{y}}_{\text{unlab}}^b$ is sampled from the relationship model $K(\hat{f}(\mathbf{z}_{\text{unlab}}^b), \hat{\phi})$. On each bootstrap sample a “regression model” is fit to the data $(\mathbf{x}_{\text{unlab}}^b, \tilde{\mathbf{y}}_{\text{unlab}}^b)$. The coefficients of this regression model, across many bootstrap samples, are used to obtain coefficient estimates and accompanying standard errors for the parameter(s) of interest.

3.2 Distribution of the test statistic of Wang et al. [2020]

In the “*Simulated Data: Continuous case*” section of Wang et al. [2020], to test $H_0 : \beta_1^* = 0$, they assume that asymptotically, $\hat{\beta}_1/\widehat{\text{SE}}(\hat{\beta}_1) \rightarrow \text{Normal}(0, 1)$ under H_0 . To determine whether this is actually the case, we create three $\hat{f}(\cdot)$ ’s, each obtained by fitting a GAM as described in Section 2.1, with a training set of 300 observations. For each $\hat{f}(\cdot)$, we conduct 1,000 simulation replicates, each consisting of a different labeled and unlabeled dataset. We see in the first three panels of Figure 3 that the empirical distribution of $\hat{\beta}_1/\widehat{\text{SE}}(\hat{\beta}_1)$, using these three $\hat{f}(\cdot)$ ’s, is quite far from $N(0, 1)$, for both the methods proposed by Wang et al. [2020] and the naive approach. In fact, the proportion of points above the top dashed line and below the bottom dashed line tells us the type 1 error rate at the level $\alpha = 0.05$: thus, this directly explains our findings in Figure 1.

Next, we set $\beta_1^* = 1$, and consider whether it is really the case that the pivotal quantity $(\hat{\beta}_1 - \beta_1^*)/\widehat{\text{SE}}(\hat{\beta}_1) \rightarrow N(0, 1)$ (since this assumption underlies the construction of confidence intervals for β_1^*). As seen in the first three panels of Figure 4, this assumed distribution is not correct for the proposal of Wang et al. [2020], or for the naive method; consequently, these two methods fail to attain the nominal coverage. In fact, we can directly read out the coverage of the confidence interval by examining the proportion of points between the two dashed lines.

We now consider the naive method in Figures 3 and 4. The distributions of both the test statistic and pivotal quantity are centered at the wrong value. To see this, recall that the naive method conducts linear regression on realizations of the random variable $(X, \hat{f}(Z))$. This regression

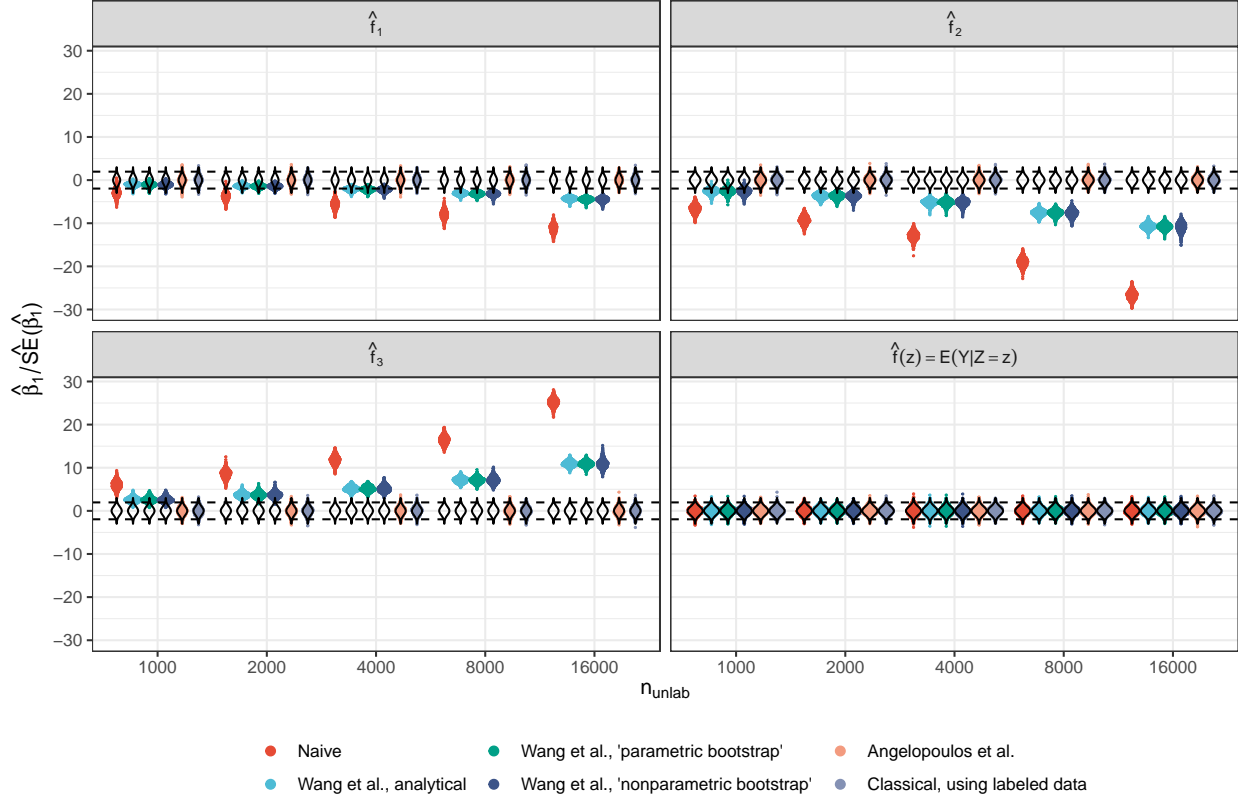


Figure 3: An examination of the distribution of $\hat{\beta}_1 / \widehat{SE}(\hat{\beta}_1)$ under $H_0 : \beta_1^* = 0$. Using three separate training sets, we generate three functions $\hat{f}(\cdot)$. For each $\hat{f}(\cdot)$, we generate labeled and unlabeled datasets, and display the empirical distribution of $\hat{\beta}_1 / \widehat{SE}(\hat{\beta}_1)$ as the sample sizes increase, with $n_{\text{lab}} = 0.1n_{\text{unlab}}$. The $N(0, 1)$ distribution is shown in black. The dashed black lines show the 0.025 and 0.975 quantiles of this distribution. The distributions of Wang et al. [2020]’s test statistics become increasingly different from the assumed $N(0, 1)$ distribution as the sample sizes increase.

targets the parameter $E(XX^\top)^{-1}E(X\hat{f}(Z))$, which is *not* equal to $\beta^* = E(XX^\top)^{-1}E(XY)$. In fact, viewing $\hat{f}(\cdot)$ as fixed (as in Figures 3 and 4), we see that the quantity $E(XX^\top)^{-1}E(X\hat{f}(Z))$ does not even involve the response, Y ; therefore, the parameter targeted by the naive method is not of any scientific interest.

Similarly, examining the bootstrap algorithm proposed by Wang et al. [2020] sheds light on the discrepancy between the observed and assumed distributions of the test statistic and pivotal quantity in Figures 3 and 4, respectively. Step 2.2 of Algorithm 1 involves sampling observations from $K(\hat{f}(Z), \hat{\phi})$ for use in fitting a linear regression model in Step 2.3. Therefore, this regression targets the parameter $E(XX^\top)^{-1}E(XK(\hat{f}(Z), \hat{\phi}))$, which in general is not equal to the parameter of interest $\beta^* = E(XX^\top)^{-1}E(XY)$. Therefore, the methods proposed by Wang et al. [2020] suffer from the same issue as the naive method: *they target the wrong parameter*.

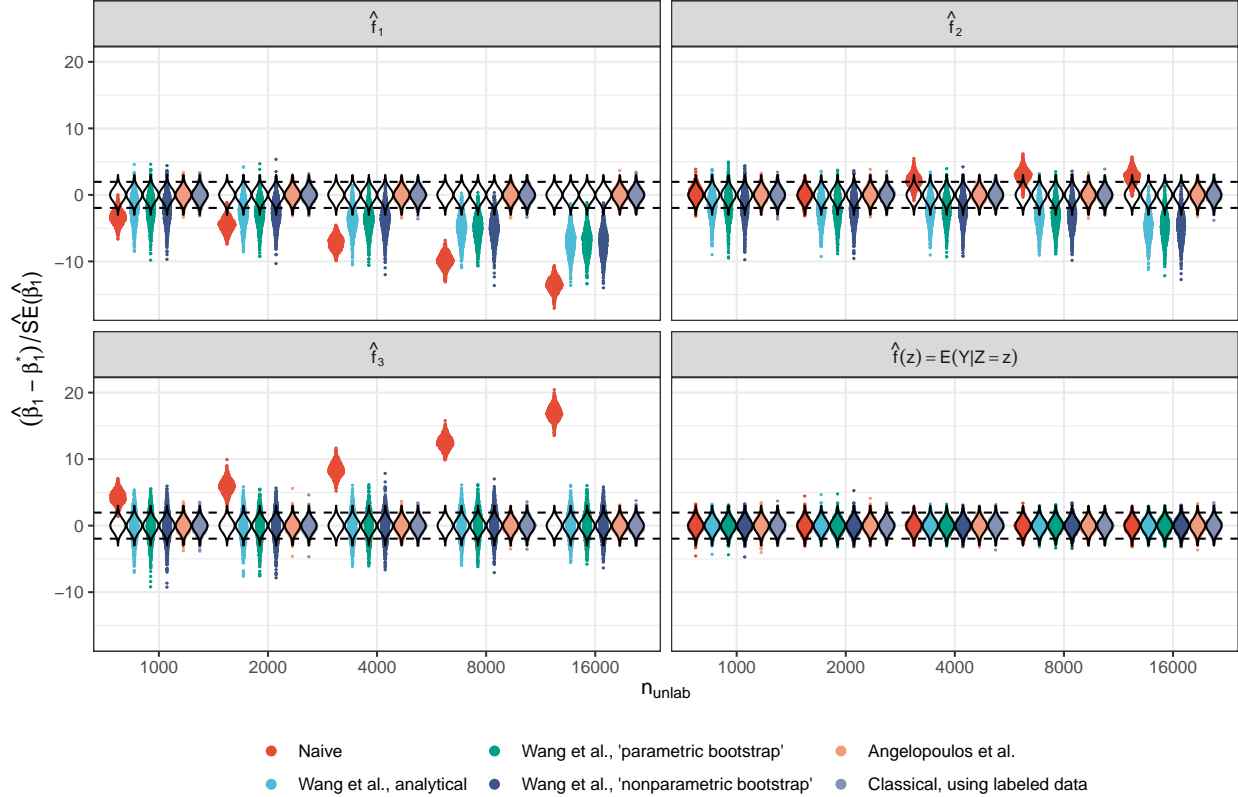


Figure 4: An examination of the distribution of $(\hat{\beta}_1 - \beta_1^*)/\widehat{SE}(\hat{\beta}_1)$ when $\beta_1^* = 1$. Using three separate training sets, we generate three functions $\hat{f}(\cdot)$. For each $\hat{f}(\cdot)$, we generate labeled and unlabeled datasets, and display the empirical distribution of the pivotal quantity $(\hat{\beta}_1 - \beta_1^*)/\widehat{SE}(\hat{\beta}_1)$ as the sample sizes increase, with $n_{\text{lab}} = 0.1n_{\text{unlab}}$. The $N(0, 1)$ distribution is shown in black. The dashed black lines show the 0.025 and 0.975 quantiles of this distribution. The distributions of Wang et al. [2020]’s pivotal quantities become increasingly different from the assumed $N(0, 1)$ distribution as the sample sizes increase, indicating that nominal coverage is not attained.

3.3 An extreme setting where Wang et al. [2020] works

We now consider an extreme setting where the prediction model *exactly* equals the true regression function, that is, when $\hat{f}(z) = E(Y|Z = z)$. In the last panel of Figures 3 and 4, we see that in this setting, the test statistics and pivotal quantities follow their assumed distributions for all methods, resulting in valid inference (see the last panels of Figures 5 and 6 in Appendix A).

It is easy to see analytically why the naive method targets the correct parameter in this extreme setting. Suppose (as in this simulation) that X is contained within Z : that is, $Z = (X, Z^{(2)})$ for some $Z^{(2)}$. Then

$$\begin{aligned}
 E(XX^\top)^{-1}E(X\hat{f}(Z)) &= E(XX^\top)^{-1}E(XE(Y|X, Z^{(2)})) \\
 &= E(XX^\top)^{-1}E(XY) \\
 &= \beta^*,
 \end{aligned}$$

showing that the naive method targets the correct parameter of interest. From the last panel of Figures 3 and 4, we see that the methods of Wang et al. [2020] similarly target the correct parameter in this extreme setting. We see this by noting that

$$E(XX^\top)^{-1}E(XK(\hat{f}(Z), \hat{\phi})) = E(XX^\top)^{-1}E(XE(K(\hat{f}(Z), \hat{\phi})|Z)) \quad (3)$$

$$\approx E(XX^\top)^{-1}E(XE(Y|Z)) \quad (4)$$

$$= E(XX^\top)^{-1}E(XY) \quad (5)$$

$$= \beta^*. \quad (6)$$

Here, (3) and (6) follow from iterated expectations since $Z = (X, Z^{(2)})$. To see why the approximation in (4) holds, recall that $K(\hat{f}(Z), \hat{\phi})$ is defined by fitting a GAM to $(Y, \hat{f}(Z))$, and adding mean-zero noise. That is, $E(K(\hat{f}(Z), \hat{\phi})|Z) := \hat{g}(\hat{f}(Z))$, where $\hat{g}(\cdot)$ is a fitted GAM, given by

$$\hat{g} \approx \arg \min_g E((Y - g(\hat{f}(Z)))^2) \quad (7)$$

$$= \arg \min_g E((Y - g(E(Y|Z)))^2) \quad (8)$$

$$= \arg \min_g E(E((Y - g(E(Y|Z)))^2|Z)). \quad (9)$$

It is not hard to see that (9) is minimized when $g(E(Y|Z)) = E(Y|Z)$, i.e., \hat{g} is approximately the identity function. Therefore, $E(K(\hat{f}(Z), \hat{\phi})|Z) = \hat{g}(E(Y|Z)) \approx E(Y|Z)$. With a large enough labeled dataset, this approximation will hold almost exactly.

However, in general, it is not reasonable to assume that $\hat{f}(z) = E(Y|Z = z)$, and in fact, our goal is valid inference on the parameter β^* regardless of (the quality of) $\hat{f}(\cdot)$. This goal is achieved by the proposal of Angelopoulos et al. [2023].

4 Discussion

In this paper, we found that the method of Angelopoulos et al. [2023] provides valid type 1 error control and coverage. By contrast, the methods proposed by Wang et al. [2020] do not provide appropriate inferential guarantees, except for under very strong assumptions: for instance, under the extreme (and unrealistic) scenario where the prediction model is the true regression function. *Under this additional assumption, the naive approach also provides valid inference.* Furthermore, we see in our simulation study that simply assuming that the prediction model $\hat{f}(\cdot)$ was trained on data from the same population as the labeled and unlabeled data — an assumption made by the original authors — is not sufficient to achieve valid inference using the methods of Wang et al. [2020].

Throughout, for simplicity we have assumed that we are conducting inference (i.e. Step 2 of Box 1) using a linear model. However, our conclusions — that the naive method and methods by Wang et al. [2020] result in invalid inference, because they target the incorrect parameter — applies much more generally. The theory in Angelopoulos et al. [2023] shows that their approach applies to a wide variety of settings beyond linear regression, and has valid inferential properties.

Code Availability

Scripts to reproduce the results in this manuscript are available at <https://github.com/keshav-motwani/PredictionBasedInference/>. This code is based on the code from Wang et al. [2020], which we thank the authors for making publicly accessible.

Acknowledgements

We thank Jeff Leek and Tyler McCormick for helpful conversations. The authors gratefully acknowledge funding from *NIH R01 EB026908*, *NIH R01 GM123993*, *NIH R01 DA047869*, *ONR N00014-23-1-2589*, and a *Simons Investigator Award in Mathematical Modeling of Living Systems*.

References

- Anastasios N Angelopoulos, Stephen Bates, Clara Fannjiang, Michael I Jordan, and Tijana Zrnica. Prediction-powered inference. *arXiv preprint arXiv:2301.09633*, 2023.
- Samuel J Clark, Tyler McCormick, Zehang Li, and Jon Wakefield. InSilicoVA: A method to automate cause of death assignment for verbal autopsy. *arXiv preprint arXiv:1504.02129*, 2015.
- Shannon E Ellis, Leonardo Collado-Torres, Andrew Jaffe, and Jeffrey T Leek. Improving the value of public RNA-seq expression data by phenotype prediction. *Nucleic Acids Research*, 46(9): e54–e54, 2018.
- Eric R Gamazon, Heather E Wheeler, Kanaan P Shah, Sahar V Mozaffari, Keston Aquino-Michaels, Robert J Carroll, Anne E Eyler, Joshua C Denny, GTEx Consortium, Dan L Nicolae, et al. A gene-based association method for mapping traits using reference transcriptome data. *Nature Genetics*, 47(9):1091–1098, 2015.
- Alexander Gusev, Kate Lawrenson, Xianzhi Lin, Paulo C Lyra Jr, Siddhartha Kar, Kevin C Vavra, Felipe Segato, Marcos AS Fonseca, Janet M Lee, Tanya Pejovic, et al. A transcriptome-wide association study of high-grade serous epithelial ovarian cancer identifies new susceptibility genes and splice variants. *Nature Genetics*, 51(5):815–823, 2019.
- John Jumper, Richard Evans, Alexander Pritzel, Tim Green, Michael Figurnov, Olaf Ronneberger, Kathryn Tunyasuvunakool, Russ Bates, Augustin Žídek, Anna Potapenko, et al. Highly accurate protein structure prediction with AlphaFold. *Nature*, 596(7873):583–589, 2021.
- SA Khoury, D Massad, and T Fardous. Mortality and causes of death in Jordan 1995-96: assessment by verbal autopsy. *Bulletin of the World Health Organization*, 77(8):641, 1999.
- Siruo Wang, Tyler H McCormick, and Jeffrey T Leek. Methods for correcting inference based on outcomes predicted by machine learning. *Proceedings of the National Academy of Sciences*, 117(48):30266–30275, 2020.

A Simulation results for a fixed $\hat{f}(\cdot)$

In this section, we slightly modify the simulation setup considered in Section 2. Specifically, in Section 2, each replicate used a different training dataset, and thus resulted in a different $\hat{f}(\cdot)$. However, in the setting of Box 2, we are primarily interested in properties of inference for an arbitrary and fixed $\hat{f}(\cdot)$, across different realizations of the data used for inference (the labeled and unlabeled datasets). Therefore, in this section, we look at the type 1 error and coverage for three distinct $\hat{f}(\cdot)$'s, each obtained by fitting a GAM on a different training dataset with sample size 300, simulated as in Section 2. In each replicate of the simulation study, we sample a new labeled and unlabeled dataset, with varying sample sizes. We also consider the oracle prediction function, $\hat{f}(z) = E(Y|Z = z)$.

In Figure 5, we see that the methods proposed by Wang et al. [2020] do not control the type 1 error rate for arbitrary $\hat{f}(\cdot)$; the situation gets worse as the sample size increases. However, the method proposed by Angelopoulos et al. [2023] does control the type 1 error rate. Wang et al. [2020] controls the type 1 error rate if the machine learning model is the true regression function $\hat{f}(z) = E(Y|Z = z)$; of course, such a perfect machine learning model is unattainable in practice.

In Figure 6, we see that the methods proposed by Wang et al. [2020] do not attain the nominal coverage for an arbitrary $\hat{f}(\cdot)$, whereas the proposal of Angelopoulos et al. [2023] does attain the nominal coverage. The naive method and the proposals of Wang et al. [2020] have appropriate coverage when $\hat{f}(z) = E(Y|Z = z)$; again, this is unrealistic in practice.

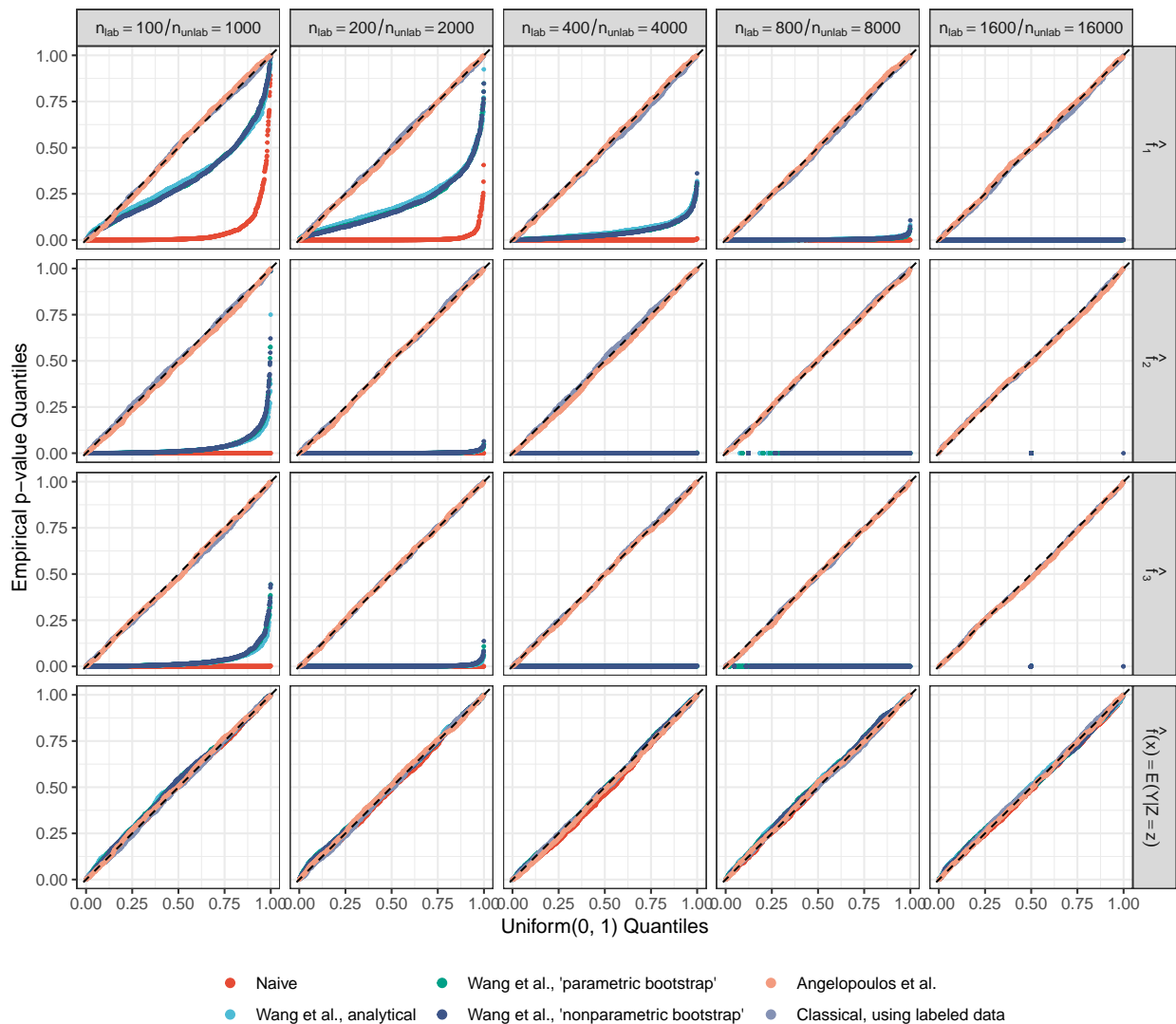


Figure 5: For labeled and unlabeled datasets generated under $H_0 : \beta_1^* = 0$, quantile-quantile plots of the p-values across replicates of the modified simulation study are displayed for each of the three $\hat{f}(\cdot)$'s considered. The methods are described in Section 2.1. Each panel corresponds to different sample sizes of the labeled and unlabeled datasets used for inference. The naive method and the bootstrap and analytical corrections considered by Wang et al. [2020] become increasingly anticonservative as the sample sizes increases, unless the machine learning model is perfect, i.e. $\hat{f}(z) = E(Y|Z = z)$.

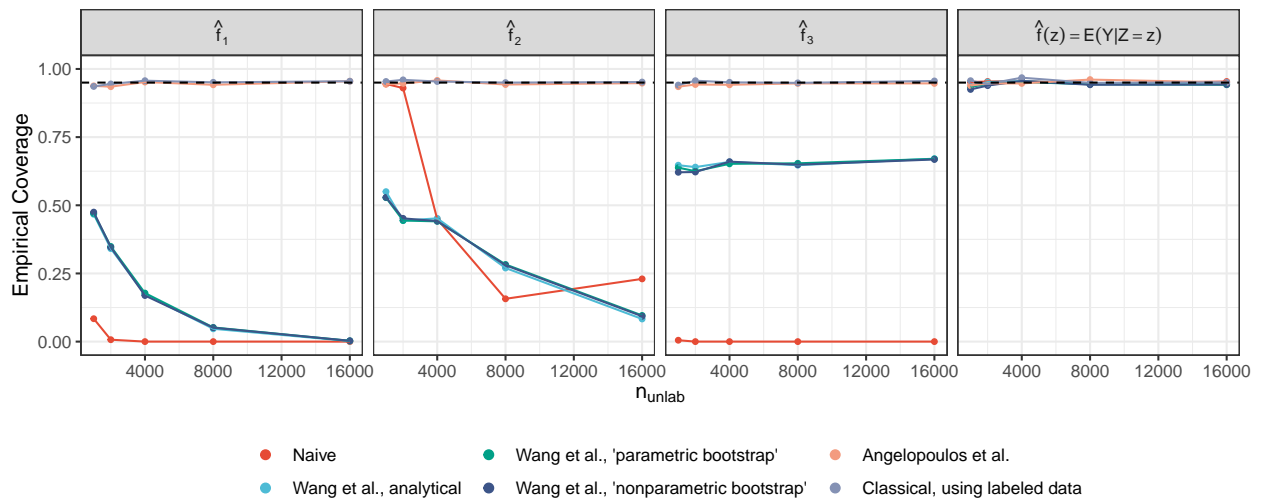


Figure 6: For labeled and unlabeled datasets generated with $\beta_1^* = 1$, empirical coverage of 95% confidence intervals for each method across each simulation replicate, for each of the three $\hat{f}(\cdot)$'s considered, as the labeled and unlabeled sample sizes increase, with $n_{\text{lab}} = 0.1n_{\text{unlab}}$. The methods are described in Section 2.1.